

PROJECT REPORT: VA163 – Part 4

ISSUE#2

Sculptor Study of a Superkart Rear Wing

PROJECT ENGINEER(S): Haakon Dahle Smith, Matthew Cross

DATE: 30 November, 2004

SIGNATURE: _____

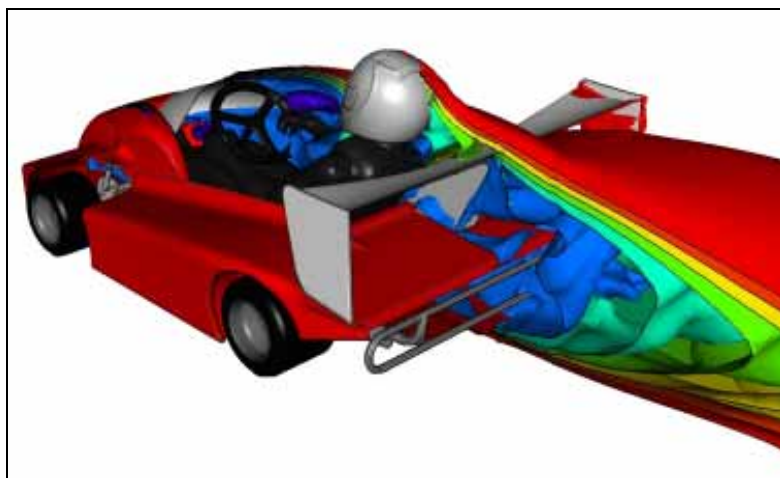
APPROVED BY: _____

REQUESTED BY: _____

SUMMARY

This report presents the results of a two-stage shape optimisation performed on the rear wing of a Superkart, which competes in the CIK-FIA European Superkart Championship. The aim of the study was to change the rear wing geometry to reduce the overall drag of the vehicle whilst maintaining the current level of downforce. Sculptor was used to make deformations to the rear wing geometry within the CFD case file. Currently, the kart uses a two-element wing. This was changed to a single element configuration to help produce a more efficient way of generating the same rear downforce.

The first stage of the process optimised the spanwise twist and scale of the airfoil section size at several spanwise locations on the wing. The second stage of the optimisation was to scale the concept from the first stage to match the same downforce as the previous two-element rear wing whilst generating less drag.



This process reduced total vehicle drag by **1.8%** whilst maintaining the current level of downforce.

CONTENTS

SUMMARY	1
1. INTRODUCTION	3
2. RESULTS	8
3. ANALYSIS AND CONCLUSION	12
4. FUTURE WORK	15
APPENDIX A: MODEL SETUP	16

1. INTRODUCTION

This report follows on from previous work carried out by Advantage CFD on a 250cc go-kart, which competes in the CIK-FIA European Superkart Championship (Figure 1.1). All of the previous CFD studies featured the two-element rear wing that is used on the kart at present. The rear wing configuration was initially changed to a single element design to produce a more efficient way of generating the same small level of rear downforce.

Figure 1.1 – Photo of kart



Figure 1.2 shows the difference in airfoil section from the two element rear wing to the new single element rear wing and Figure 1.3 identifies the new rear wing.

Figure 1.2 - Difference between biplane and monoplane rear wing

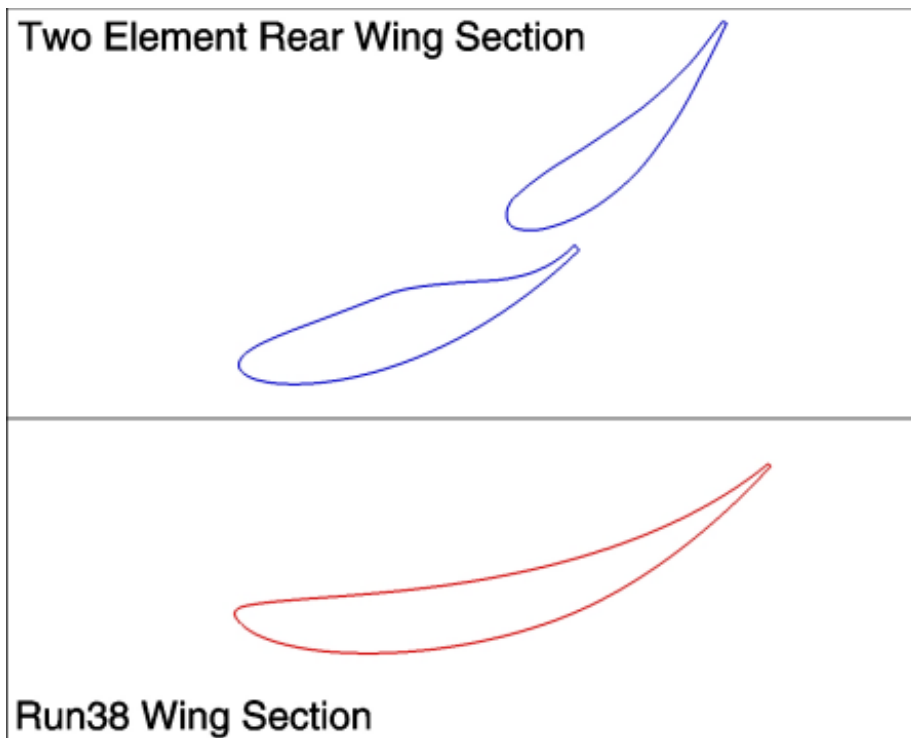
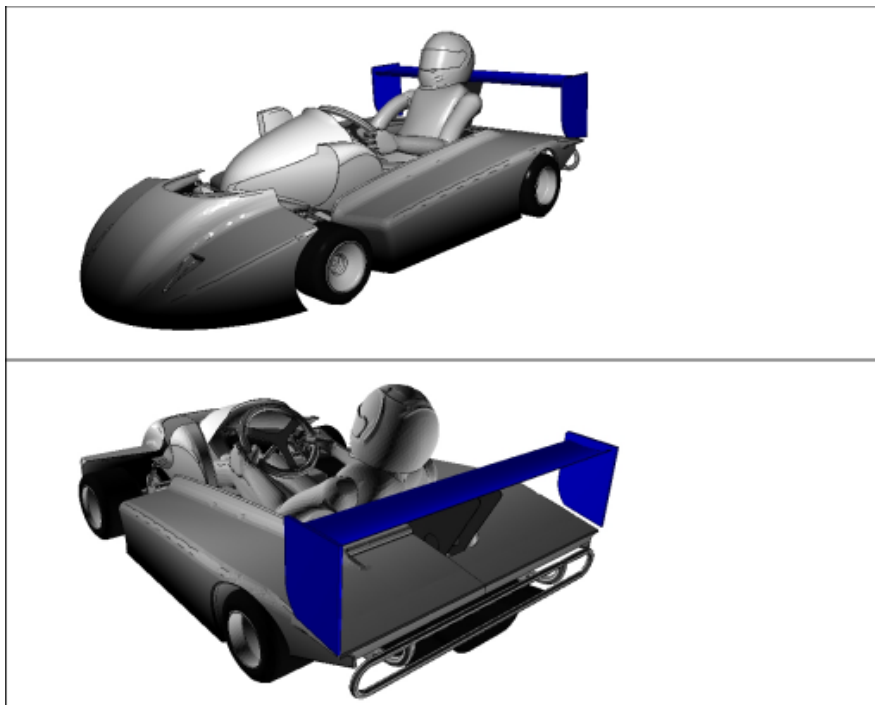
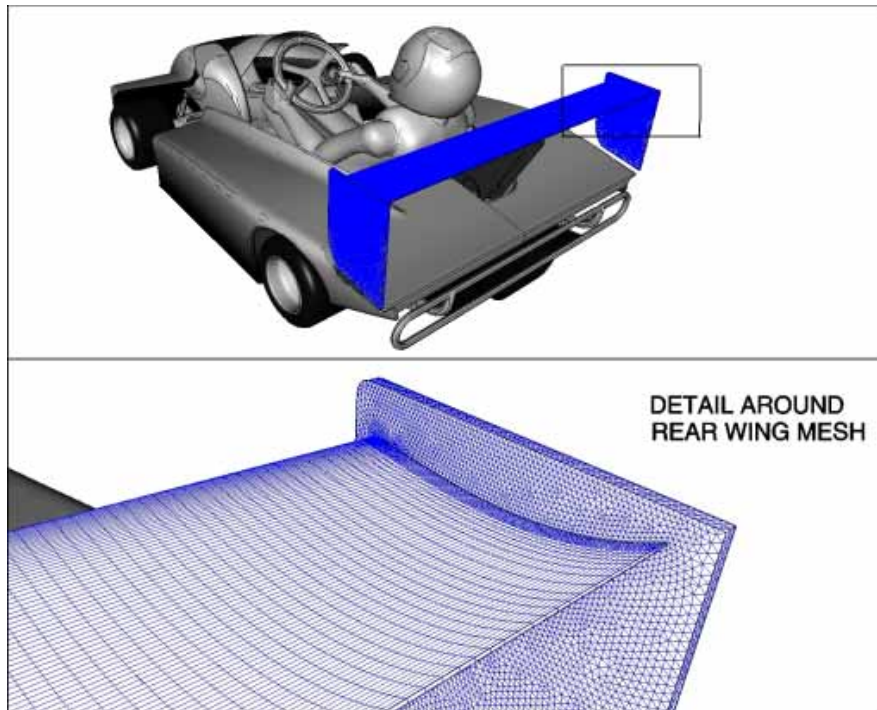


Figure 1.3 - CAD geometry of kart with blue rear wing



A 3.7 million cell hybrid mesh was used with hexahedra on the rear wing, diffuser and between the underfloor and ground. A detailed view of the rear wing mesh used is shown in Figure 1.4.

Figure 1.4 – Superkart surface mesh



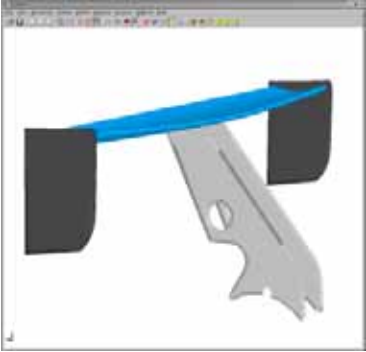
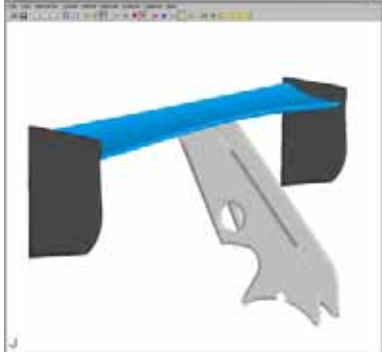
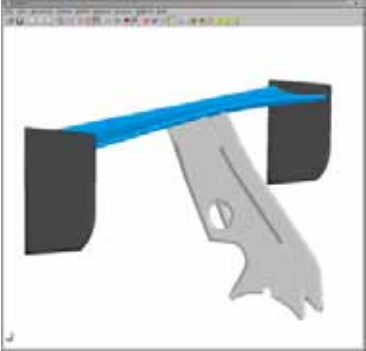

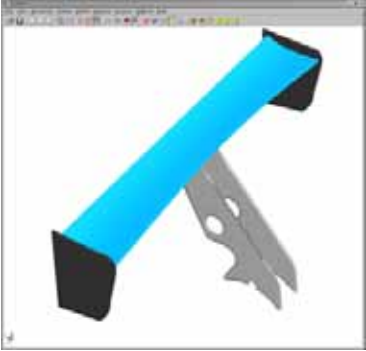
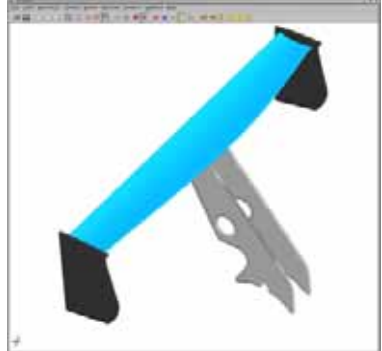
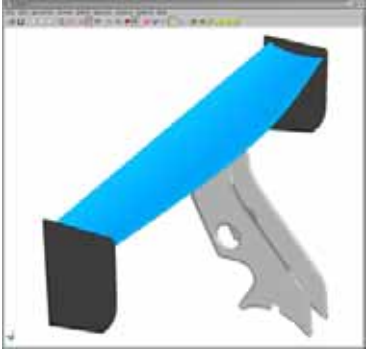
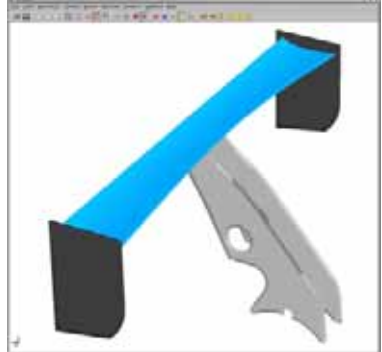
Sculptor was then used to deform the new single element rear wing geometry directly without the need to re-mesh.

The following four parameters were used as part of the study:

- Angle of attack of outboard section
- Angle of attack of the inboard section
- Section size of the outboard section
- Section size of the inboard section

An overview of the deformations that were carried out is shown visually in Figure 1.5 and an [MPEG movie of the deformations](#) can be viewed on the electronic copy. Once these parameters had been defined in Sculptor the deformations could be made interactively – directly to the case file. Note that Figure 1.5 shows the limits used (outer bounds) used in the study.

Figure 1.5 - The maximum and minimum deformations of the 4 parameters

Deformation	Maximum Deflection	Minimum Deflection
Angle of attack of outboard section		
Angle of attack of the inboard section		
Section size of the outboard section		
Section size of the inboard section		

The man-time required to produce these cases in Sculptor was very small in proportion to the computational time taken to solve the case. The initial definition of the changes took approximately 4-5 hours to setup, thereafter each change in the geometry only took 4-5 minutes.

As Sculptor maintains the same connectivity for each case the single element baseline data file was used as a starting point for the solution and only required a further 1000 more to converge as opposed to the previous 3000 iterations required to converge the baseline.

2. RESULTS

A response surface methodology was employed which required 25 initial runs to define the relationship between the four parameters and the performance function. These preliminary results are shown in Figure 2.1. Figure 2.2 shows the difference between each case and the single element baseline in terms of downforce and drag

Figure 2.1 – Total downforce for each of the initial experiments

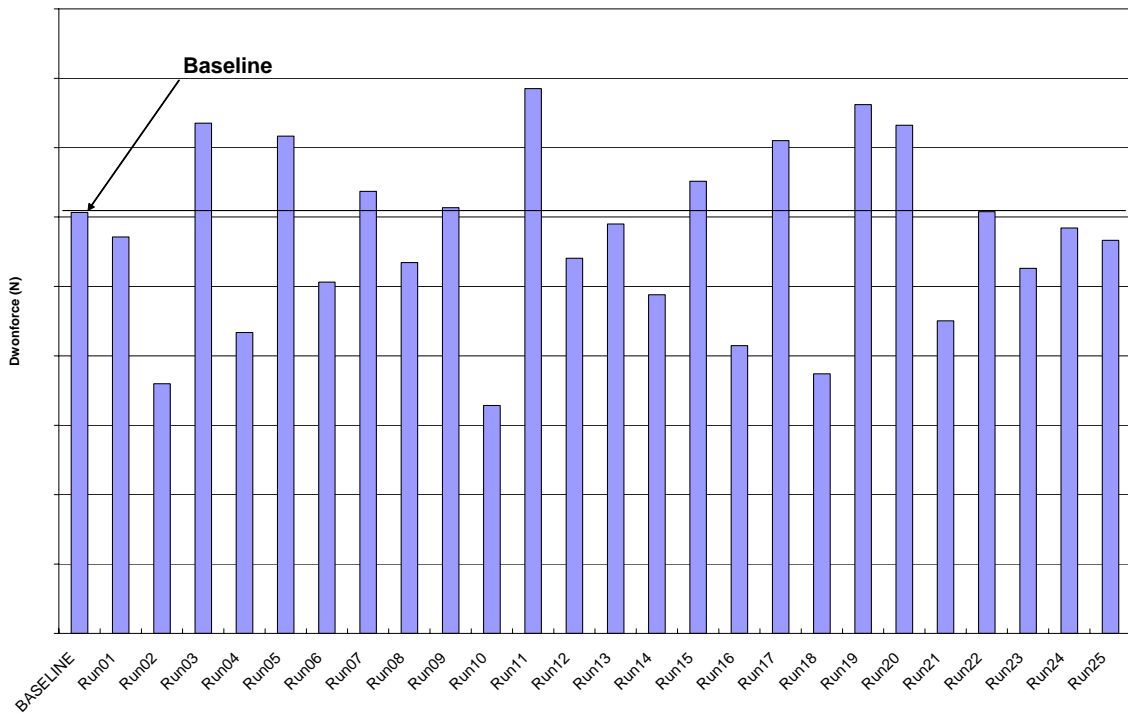


Figure 2.2 - Graph showing data points and trend line for performance function

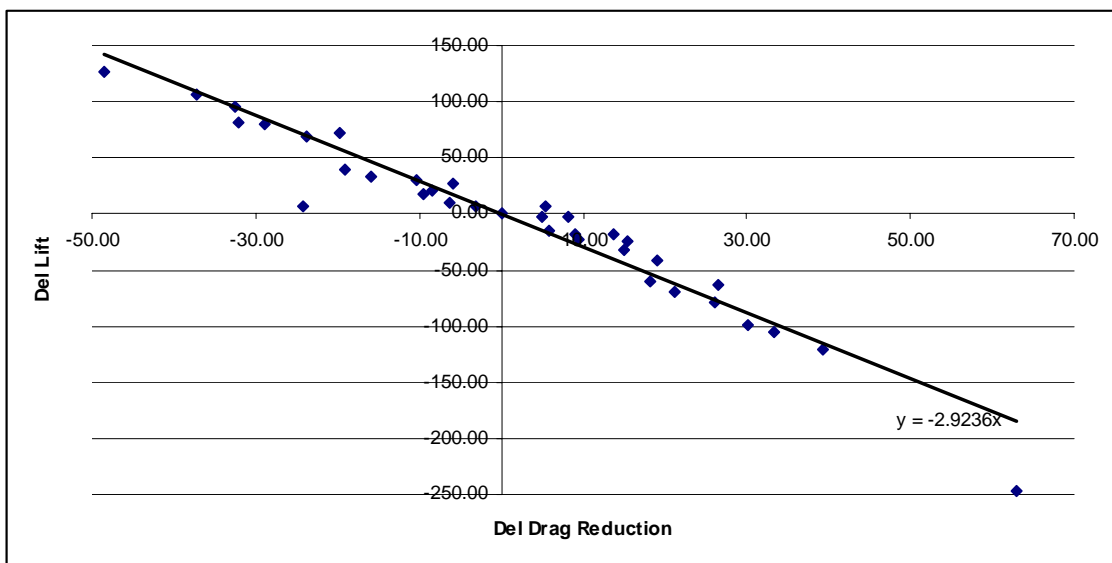


Figure 2.2 shows that there is an almost linear relationship between downforce and drag for all of the changes. This means that a simple performance function such as a minimum drag could not be used. In addition it was not possible to use efficiency as an accurate metric. In this case wings that generated a large amount of downforce resulted in a more efficient vehicle (as the rear wing is an efficient method of generating downforce compared to the rest of the Super-kart) and the design goal was a more efficient rear wing for the same level of rear downforce. Therefore a performance function was needed that was more than a simple lift or drag measure.

Initially a least squares regression line was fitted through the data shown in Figure 2.2. This defined an ‘average’ relationship between delta-drag and delta-downforce for this set of experiments.

By assuming that for each wing concept this ‘average’ relationship would stay approximately the same as the wing is scaled up or down it is possible to estimate the change in drag for the **same** total downforce for each design. This is shown diagrammatically in Figure 2.3 (single element baseline = blue, Run_x = red). Figure 2.4 plots the performance function over the initial 25 runs.

Figure 2.3 - Diagrammatic representation of performance function

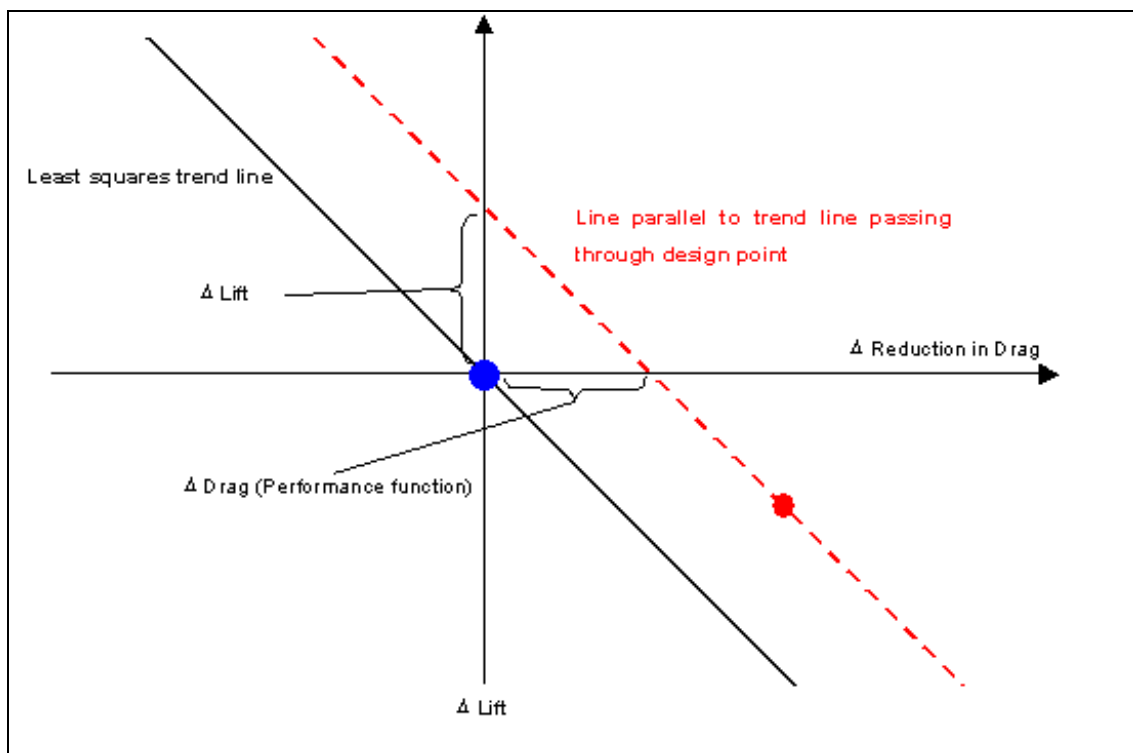
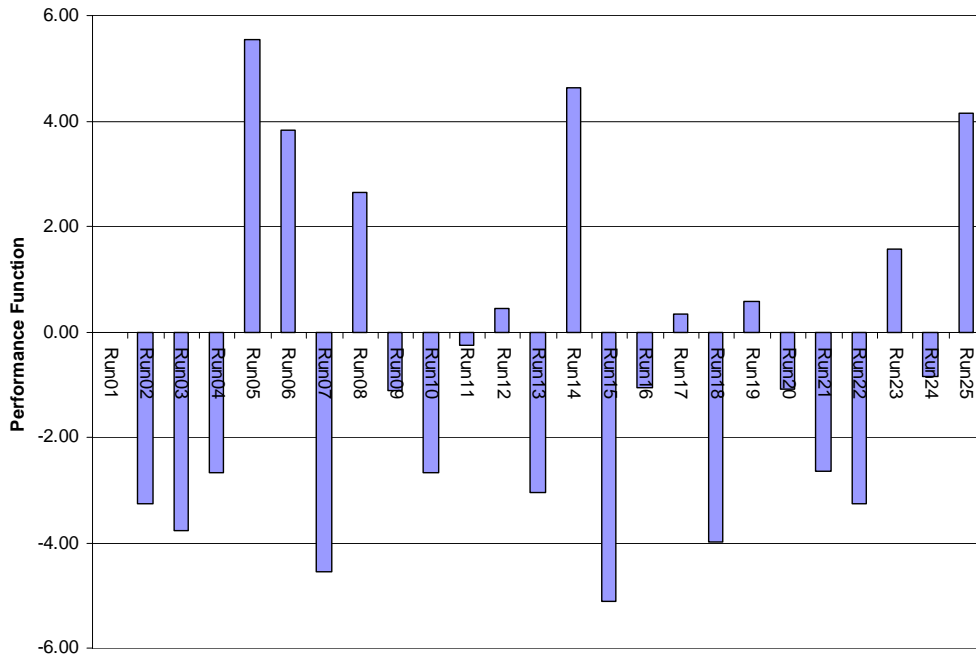
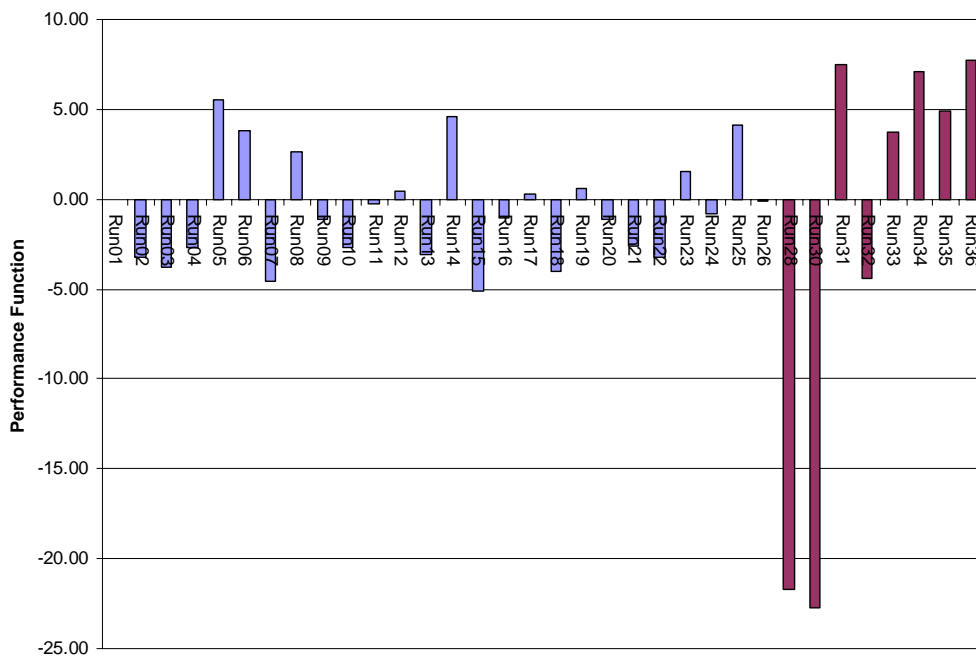


Figure 2.4 - Variation of performance function over initial runs



A further 9 cases were then needed to further populate the design space and find the optimum with this response-surface method based on this performance function. The value of the performance function for these 9 extra runs is plotted in Figure 2.5 along with the initial 25 runs.

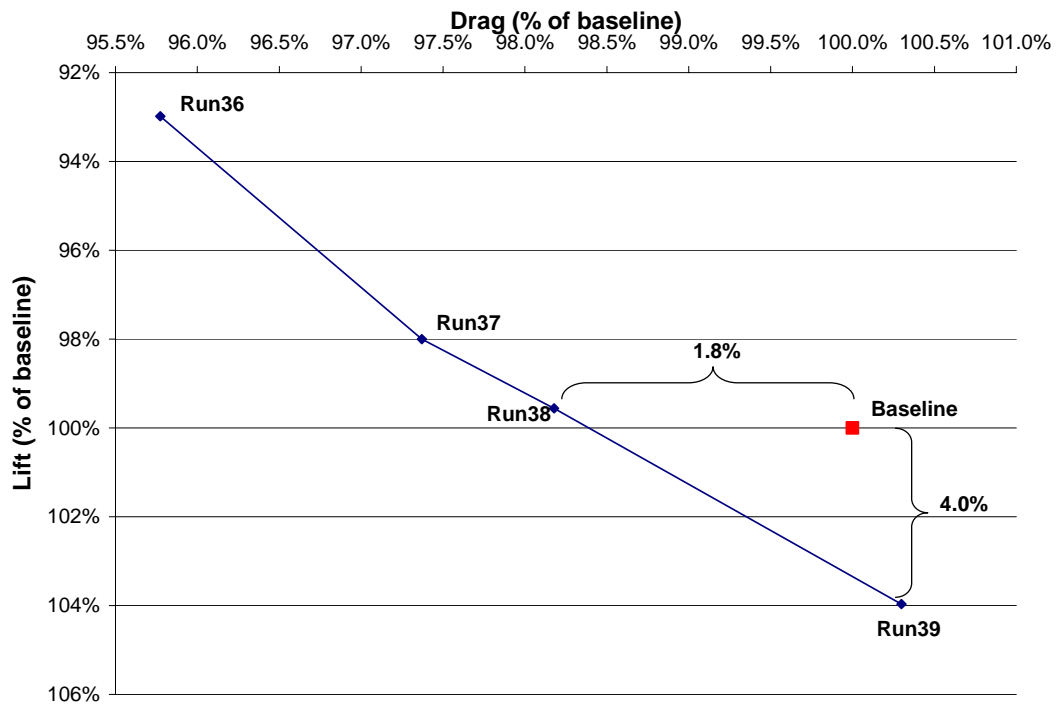
Figure 2.5 - Variation of performance function over all runs



The results of these additional cases showed that Run 36 returned the best value of the performance function but as can be seen from Figure 2.6, Run 36 produces 4.3% less downforce.

Figure 2.6 also shows the results of an additional 3 runs (all of which were scaled up versions of Run 36 in order to physically adjust the downforce level)

Figure 2.6 - Plot of lift against drag for the 2nd phase of optimisation



3. ANALYSIS AND CONCLUSION

Figure 2.6 shows that for the same level of downforce (Run 38) the new design reduces drag by 1.8%. Alternatively, a 4% gain in downforce is possible for the same level of drag (Run 39). All of these designs are achieved by scaling Run 36 to meet the requirements. For example the chord of Run 38 is 16% larger than that of Run 36.

The difference between the geometry of Run 38 and the baseline single element rear wing can be found in Figure 3.1 and a variation in spanwise section is shown in Figure 3.2. It can be seen that the outboard sections have a longer chord than the inboard sections and have a reduced angle of attack. The inboard sections have a reduced chord and an increased angle of attack.

This configuration may increase the pressure gradient towards the centre of the wing section and reducing the strength of the tip vortices and therefore reducing the drag.

Figure 3.1 - Change in rear-wing from baseline to Run38 (Front View)

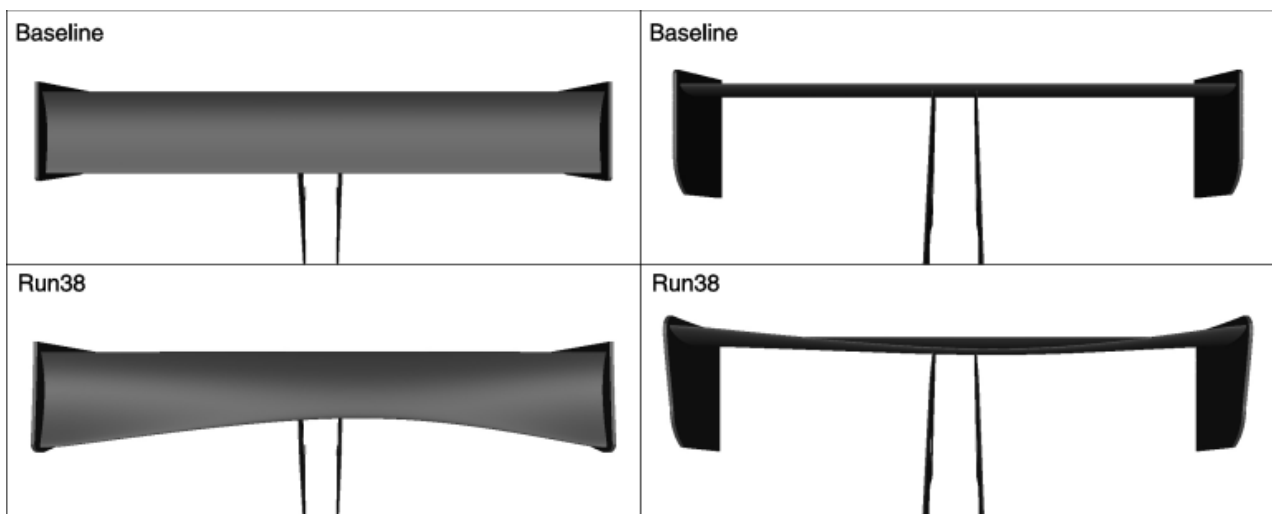
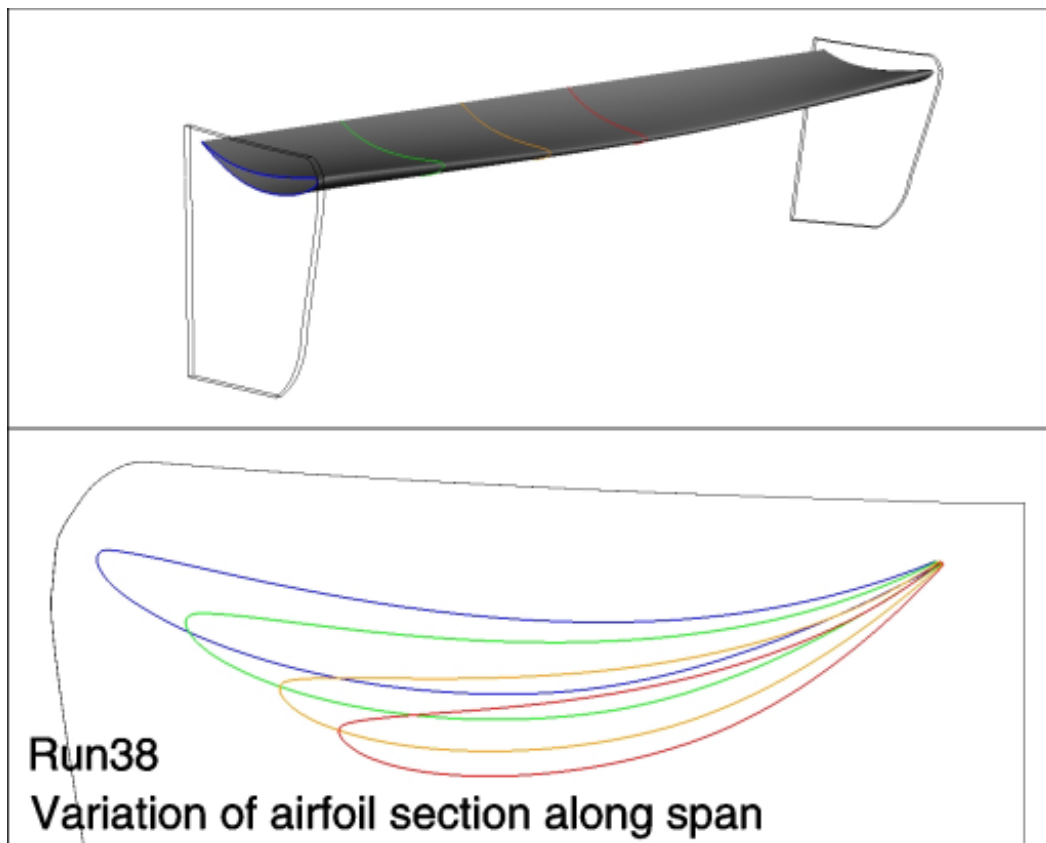


Figure 3.2 - Difference in airfoil section size and angle of attack across span of Run 38



An MPEG [movie showing the change in airfoil section shape](#) and pressure coefficient variation across the span for both optimised and baseline two-element wing can be found in the electronic copy of this report.

Figure 3.3 shows the spanwise C_{Lc} (spanwise lift loading of the rear wing) for the following runs:

- Baseline (two-element)
- Baseline (single-element)
- RUN 38

This plot shows that the optimised RUN 38 has higher lift coefficient in the centre sections of the wing whilst it has less loading at the tips confirming the reduction of the tip vortex (and associated drag).

Figure 3.3 - Plot of spanwise C_{Lc} for Baseline, RUN 38 and 2-Element-Baseline

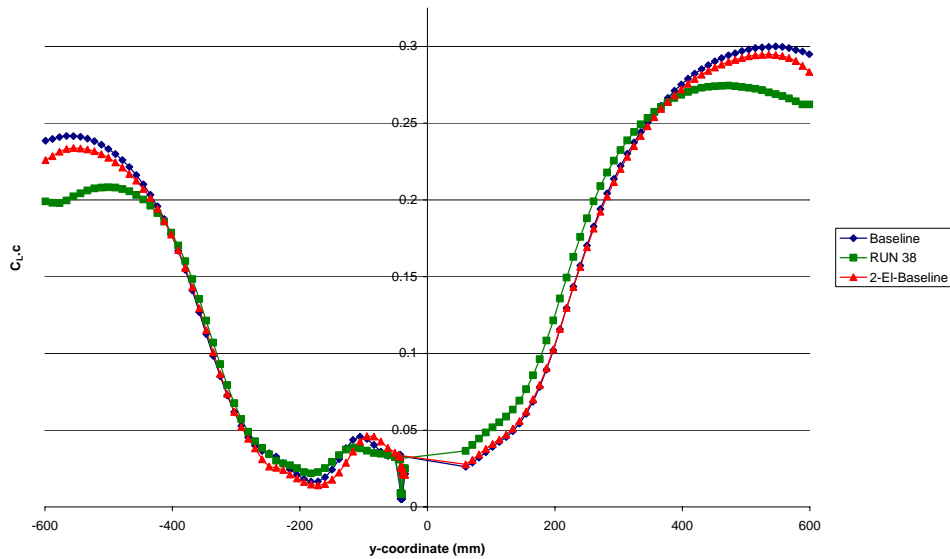
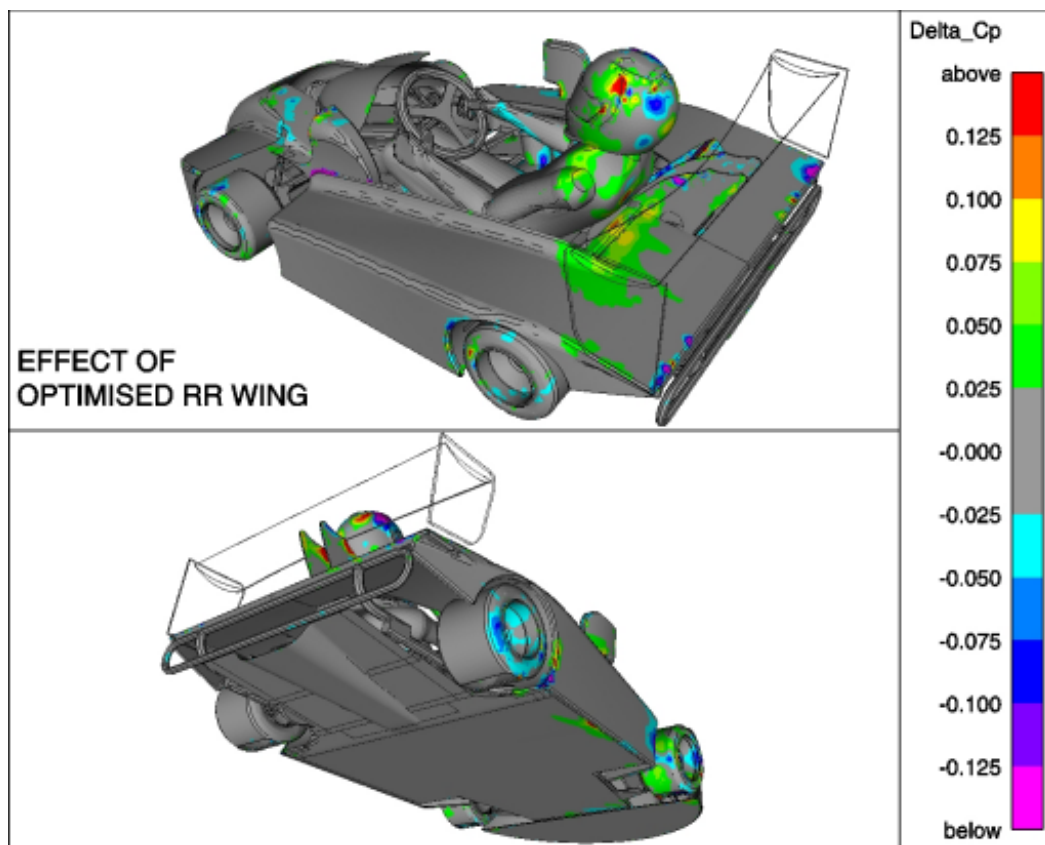


Figure 3.4 shows the go-kart coloured by the change in surface static pressure coefficient between Run38 and the two element baseline wing. Regions of the bodywork where the pressure is lower in RUN 38 than the baseline are shown in blue/purple. Areas where the pressure is higher are shown in green/red.

It can also be seen that there are very few differences between the two cases apart from the drivers left hand side and the bodywork directly behind this. This indicates that there is minimal interaction between the rear wing and the rest of the vehicle or driver.

Figure 3.4 - Superkart coloured by change in pressure coefficient



4. FUTURE WORK

Further work to be investigated could take the form of:

- A different Sculptor ASD volume, which would deform the rear wing differently or with different parameters
- Validate the reports findings through manufacture of the rear wing and subsequent test.
- Optimisation on other components e.g. radiator ducts, sidepod etc.

APPENDIX A: Model Setup

GENERAL DETAILS	
Case & Data file(s)	RunXX.cas
Mesh Type (if hybrid - areas of hex)	Hybrid Rear-wing
Number of cells	3.7e06
SOLVER CONTROLS	
Turbulence Model	Spalart-Allmaras
Near-wall Treatment	Log-law-of the wall
Discretization (Under-relaxation)	
Pressure	2 nd Order (0.3)
Momentum	QUICK (0.7)
Pressure-Velocity Coupling	SIMPLE
Turbulence	QUICK (0.8)
Buoyancy forces	Off
MATERIALS	
Density	1.225 kg/m ³
Viscosity	1.7894e-05 kg/ms
BOUNDARY CONDITIONS	
Main Inlet	53.33m/s
	Turbulence intensity 0.24%; Hydraulic diameter 0.1m Dir ⁿ vector (1, 0, 0)
Ground	As main inlet
Front Wheel	
Case A :	Axis (0, 1, 0); Centre (right) (-1.112, 0.512, 0.130) $\omega = 410.23$ rad/s
Rear Wheel	
Case A :	Axis X=0.9133, Centre (right) 0, 0.5145, 0.140) $\omega = 380.93$ rad/s